Green Production of Lead-free BZT-BCT Thin Films for Applications in MEMS Devices

Paola S. Barbato[a,*], Valeria Casuscelli[b], Paolo Aprea[a], Rossana Scaldaferri[b], Immacolata Pedaci[b], Domenico Caputo[a]

[a]ACLabs - Laboratori di Chimica Applicata, DICMaPI, Università degli Studi di Napoli Federico II, P.Le V. Tecchio 80, 80125 Napoli
[b]Analog, MEMS & Sensors Group STMicroelectronics, Via Remo De Feo, 1 80022 Arzano, Italy
paolasabrina.barbato@unina.it

This paper reports the production of Lead-free $(1-x)(BaZr_{0.2}Ti_{0.8}O_3)$-$x(Ba_{0.7}Ca_{0.3}O_3)$ ferro/piezoelectric thin films by means of repeated chemical solution deposition routes. Two different kinds of precursor solutions were compared: i) a literature standard precursor solution involving the use of 2-methoxyethanol (2-MOE) which is a toxic and carcinogenic solvent and ii) a "greener" precursor solution based on 1-methoxy-2-propanol (PGME), a non-toxic and non-carcinogenic solvent. Morphology, crystal structure and ferroelectric behavior of the films is also reported.

1. Introduction

With the advent of the 4th industrial revolution, the use of microelectromechanical systems (MEMS) in sensing applications for the detection of physical parameters (temperature, humidity) and human motion, is constantly increasing (Trolier-Mckinstry and Muralt, 2004). The majority of MEMS devices are constituted by piezoelectric thin films (Trolier-Mckinstry and Muralt, 2004). The integration of thin films in MEMS devices is essential to have a series of advantages, such as small weight and inertia, low power consumption and short response time (Hu, 2018).

Up to date, lead zirconate titanate (Pb $ZrxTi1-xO_3$), commonly known as PZT, is by far the most used ferroelectric-piezoelectric ceramic both in bulk and thin film form, despite its PbO content is about 70%wt (Shen and Liu, 2018). Unfortunately, during the production and use of PZT, a series of toxic substances, which are detrimental for the environment, are produced (Shen and Liu, 2018). This fact poses a serious concern about the environmental impact of both the synthesis process and the use of such material.

Nowadays, to reduce the environmental pollution, lead-free materials are being extensively investigated to replace PZT. The most studied families of lead-free ferroelectric-piezoelectric materials are those with a structure: (1) sodium potassium niobate($K_{0.5}Na_{0.5}NbO_3$, KNN), (2) bismuth sodium titanate ($Bi_{0.5}Na_{0.5}TiO_3$, BNT), and (3) barium zirconate titanate – barium calcium titanate ($x(BaZr_{0.2}Ti_{0.8}O_3)$-$(1-x)(Ba_{0.7}Ca_{0.3}O_3$, BZT-BCT) (Malic 2018, Barbato 2019).

Among these materials, BZT-BCT shows a response comparable or, in certain cases, higher than that of PZT, even if in a narrower range of temperature (<110°C), representing a promising PZT substitute, especially for sensors working at room temperature.

Concerning the synthesis methods of ceramic thin films, the sol-gel technique (Aprea, 2017, Shen and Liu, 2018), also known as Chemical Solution Deposition, is of a great importance, and therefore widely used, thanks to the possibility to finely tune the stoichiometry, which is particularly important for such kind of perovskitic materials having a quite complex formula. Moreover, this technique usually involves moderate synthesis temperatures with respect to solid state reaction method. However, harmful solvents, such as 2-methoxyethanol (2-MOE), are typically used in the starting solutions containing metals precursors (salts and alkoxides) and constitute the literature standard for this kind of materials (Malič,2018). The choice of the appropriate solvents appears then crucial to improve the environmental sustainability not only of the final material but also of the entire production process. In this work, in order to assess the feasibility of an
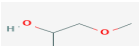
alternative process based on a more environmentally friendly solvent, namely 1-methoxy-2 propanol (also known as PGME), a precursor solution containing PGME was prepared and deposited over platinum-coated silicon wafer. The results were compared with respect to the standard procedure containing the 2-MOE solvent.

2. Materials and Methods

2.1 Precursor solution synthesis and characterizations

The procedures to produce the 2-MOE-based precursor solution and the PGME-based precursor solution are quite similar and schematically reported in Figure 1. Table 1 reports the main physical properties of the two solvents, indicating the reasons, which guided the selection of PGME as an alternative solvent: it is evident that the solvent share very similar structure and properties.

Table 1: Physical properties of the solvents

Solvent	IUPAC name	Formula	2D Structure	Boiling point °C	Surface Tension mN/m	Hazard statements
2-MOE	2-Methoxyethanol	$C_3H_8O_2$		125	30.84	H226 - H302 + H312 + H332 - H360FD - H370 - H373
PGME	1-Methoxy-2 Propanol	$C_4H_{10}O_2$		120	27.7	H226-H336

As metal sources, barium acetate ($Ba(CH_3COO)_2$,) calcium acetate monohydrate ($Ca(CH_3COO)_2 \cdot H_2O$), zirconium propoxide ($Zr(OCH_2CH_2CH_3)_4$,) 70% solution in 1-propanol, tetrabutyl titanate ($Ti(OC_4H_9)_4$) were used. Ethylene glycol (EG) and glacial acetic acid (HAc) were used as co-solvent and chelating agents. All the chemicals were of analytical grade and were used without further purification.
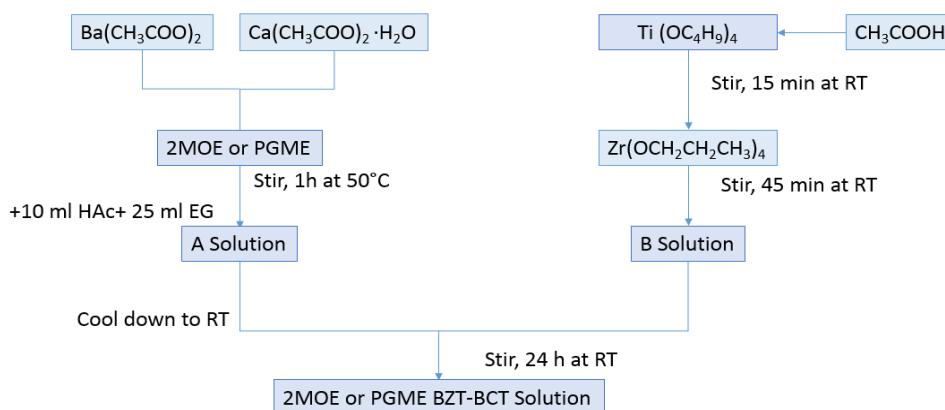

Figure 1: Precursor Solution Synthesis

To produce the A solution, barium and calcium acetate were mixed and shaken with 2-MOE or PGME in a water bath at T = 50°C; after 40 minutes the solution was still opalescent, indicating the presence of acetates not dissolved. To solve all residuals, 10 ml of acetic acid and 25 ml of ethylene glycol were added, and a clear solution was obtained. This mixture was cool down before to mix with solution B.
Solution B was produced by dissolving tetrabutyl titanate in acetic acid and shaking at room temperature for 20 minutes, then adding zirconium propoxide and shaking for 1 hour.Solution A and solution B were mixed and shaken for 24 h at room temperature to obtain a clear solution of BZT-BCT 0.2 M in 2-MOE or in PGME. From here on, the solutions will be denoted with the abbreviation of the solvent used.
 About 15 ml of the 2-MOE and PGME precursor solutions were dried at 120°C, which resulted in precipitate gel formation. Afterwards, the obtained powders were grounded and calcined at 1200°C to induce the formation of BZT-BCT.
The crystal phase of the powder after the calcination process was studied by X-ray diffraction technique (PANalytical, X'Pert Pro).

White precursor powders derived from the gel were thermally analyzed by High temperature Differential Thermal/Thermogravimetric Analysis (NETZSCH, STA 409 Luxx). The temperature was scanned from room temperature to 1200 °C at a heating rate of 10°C/min under nitrogen flow.

2.2 Thin films deposition and characterizations

The deposition, drying and pyrolysis steps were carried out in a glove box. The precursor solutions were deposited onto $Pt/TiO_2/SiO_2/Si$ substrates by spinning it in a spin coater (Specialty Coating Systems, model P.6712), according to a three-stage spinning program. The films were then thermally treated in a rapid thermal annealing furnace (RTP) in O_2 flow at 830°C for 60 sec. The process was repeated to obtain films with 4 layers (one layer deposition followed by RTP + three layers deposition followed by RTP). The temperatures of the first and second hot plates were fixed at 150°C and at 450°C, respectively. From here on the 4 layers thin films will be denoted as "1+3L name of solution" sample.

The crystal structure of the deposited oxide was checked by X-ray powder diffraction (XRPD, PANalytical X'Pert Pro automated diffractometer equipped with a XCelerator PIXCEL 1D detector) in grazing incident diffraction (ω = 1°) over a 2θ range from 10 to 40°, with the following operating conditions: CuKα radiation, 40 kV, 40 mA, step size 0.0131° 2θ, counting time 18.87 s per step. Surface features of BZT-BCT samples at micro- and nano- scale, such as surface roughness and texture uniformity, were evaluated from images collected by a scanning electron microscope (SEM). SEM images were performed at an accelerating voltage of 10 kV with a working distance of 5 mm and aperture of 30 μm by using a field emission gun (FEG) microscope Carl Zeiss, SUPRA 40. FEG microscopes can operate at very low accelerating voltages allowing to measure also insulating materials without any metal coating. Finally, BZT-BCT thin films were characterized in capacitors structures with platinum electrodes. Devices were realized by sputtering top electrodes through a shadow mask onto the film surfaces, to obtain a final stack $Si/SiO_2/TiO_2/Pt(100nm)/BZT$-BCT thin film/Pt(100nm). The contact with Pt bottom electrode was provided by manually etching the film layer with HCl 1M at 100 °C. The electrical characteristics of such devices were measured at room temperature by Aixact TFAnalyzer 2000E.

3. Results

3.1 Precursor solutions

X-ray diffraction pattern of BZT-BCT precursor powders after the calcination process show the characteristic peaks of perovskite single-phase in both cases (Figure 2).
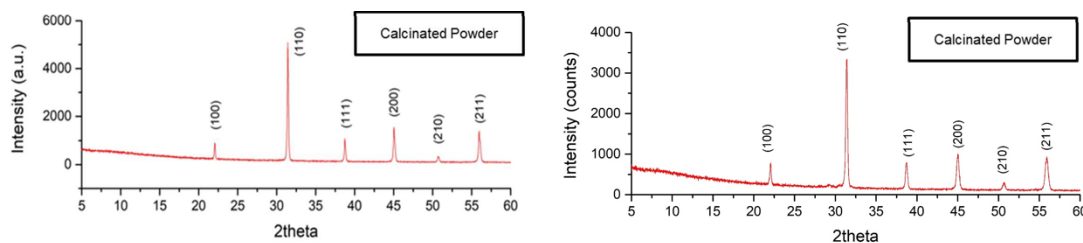

Figure 2: XRD on calcinated powders deriving from: a) 2-MOE solution; b) PGME solution

The TG analysis is visually reported in Figure 3 and numerically reported in Table 2. It appears that the two precursor solutions behave very differently: the thermal behavior of the 2-MOE solution is more complicated, accounting more than six different peaks. According to the work of Wang (2013) and Aprea (2017), the first two peaks (i.e. in the range of temperature <250°C) can be attributed to the evaporation of residual solvent or alcohols produced by condensation reactions during gel formation. The third and fourth peaks are in the range which extends up to 600°C and are related to the decomposition of xerogel with the loss of organic matter, the formation of titanium and zirconium oxides and the decarboxylation of acetates to produce $BaCO_3$ and $CaCO_3$. The last peaks are attributable to crystallization of BZT-BCT perovskite.

What was above explained in the case of 2-MOE solution is valid also in the case of PGME solution, the main differences being the number of peaks, that in the PGME are three. The first two peaks appear in the 250°C-600°C range and the last (at 1021 °C) is related to BZT-BCT crystallization.
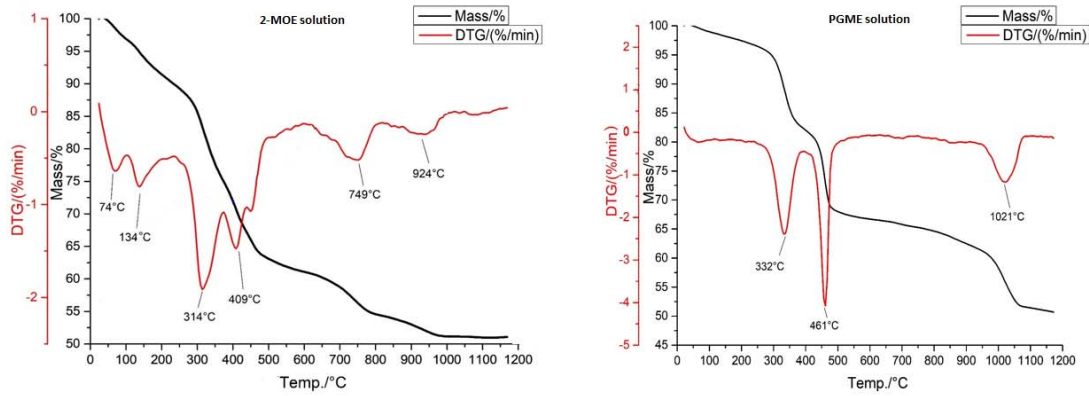
Figure 3: TGA and DTG on dried powders: a) 2-MOE solution; b) PGME solution

The yield upon drying was calculated according to eq. (1) and reported in Table 2.

$$Yield = \frac{Weight\ of\ dried\ powders}{volume\ of\ solution} = \left[\frac{g}{ml}\right] \tag{1}$$

Table 2: Yield upon drying, and weight lost during TG-DTG analysis

Precursor powders	yield, g/ml	Weight loss, %			Total weight lost, %
		T<250°C	250°C<T<600°C	T> 600°C	
2-MOE	0.089	10	30	10	50
PGME	0,085	5	30	15	50

3.2 Thin films

As reported in Table 3 the thickness of the 4-layer thin films is about 140nm and 120 nm for the 1+3L 2-MOE and 1+3L PGME, respectively. The crystalline structures of 1+3L "MOE and 1+3L PGME BZT_BCT thin films are reported in Figure 5 a) and b), respectively. XRD data on thin films suggest, according to the work of Khang (2012) and Lin (2012), a non-oriented perovskite structure. Peaks at 22°, 32° and 38° are visible with 2θ scan at ω=2°. Peaks at 26° and 36° are referred to Si-TiO$_2$-Pt substrate.

Table 3: Thickness and Ferroelectric results of the thin films

Sample	Thickness, nm	Pr µC/cm^2	Ec, kV/cm	E
1+3L 2-MOE	140	5.24	147. 6	265.5
1+3L PGME	120	4,89	236,4	196.0

SEM images, in Figure 6 at 10 KX magnification, exhibit homogeneous structure on micrometric scale with the presence of a reticular structure; increasing the magnification at 500KX, the images show a two-phase structure, but also pores with a diameter of ~ 15 nm in the 1+3L 2-MOE sample. The average diameter of crystalline grains is ~25-30nm for the 1+3L MOE thin film and ~20nm for the 1+3L PGME thin film. Hysteresis study was performed on capacitors at room temperature, as shown in the Figure 7. P-E data are taken at a constant measurement frequency of 1 kHz and 10V. It appears that both thin films behave similarly as ferroelectrics. From these curves it is possible to obtain the remnant polarization (Pr) and coercive fields (E$_c$) which values are summarized in Table 3 together with the dielectric constant (ε) values evaluated from Capacitance Voltage measurements (not shown).
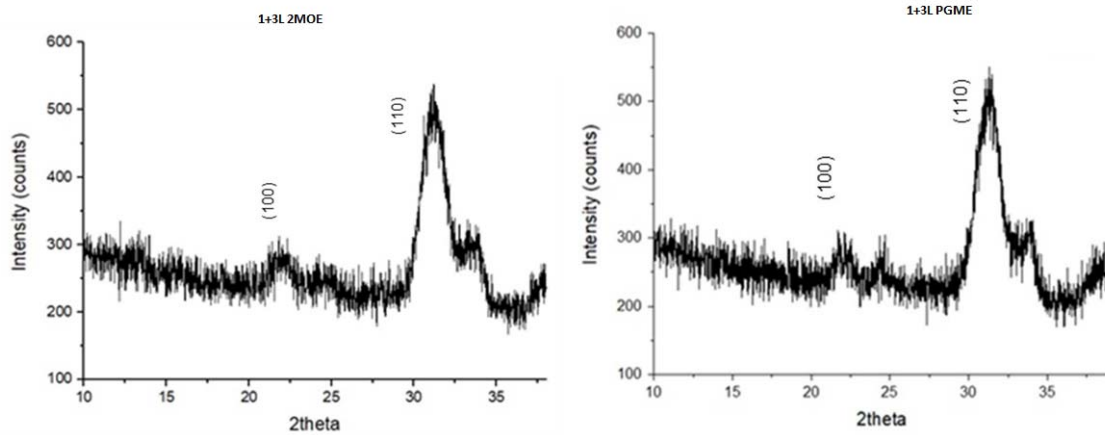
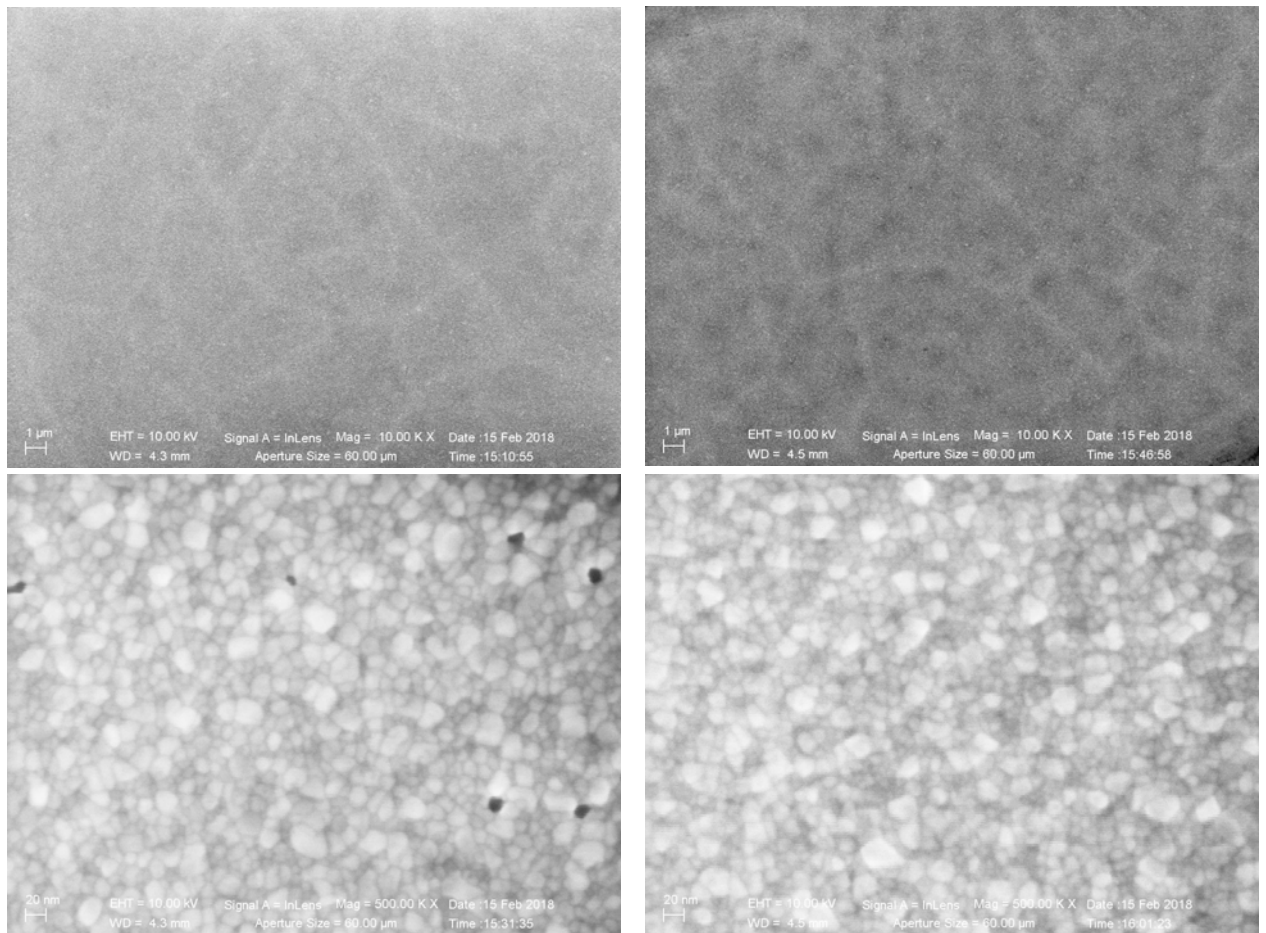*Figure 5: XRD pattern of 4-layer BZT-BCT films: a)1+3L 2-MOE; b) 1+3L PGME*

Figure 6: SEM images of BZT-BCT films: a)1+3L 2-MOE (10KX); b) 1+3L PGME (10KX); c) 1+3L 2-MOE (500KX); d)1+3L PGME (500KX)

The best results are obtained for the 2-MOE thin films both in terms of P_r, which is the highest, and in terms of E_c, which is the lowest according to the highest dielectric constant. This is due to: i) the higher thickness, for which the clamping effect of the substrate is less important (Kang, 2012), and ii) the bigger grains.
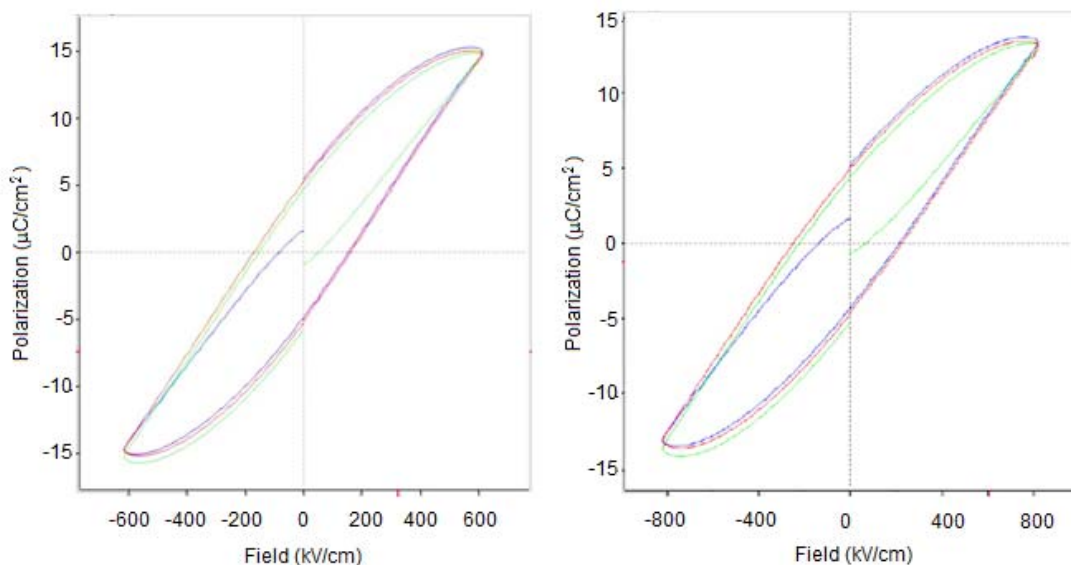
Figure 7: Hysteresis loop of BZT-BCT with 10V of applied field and 1 kHz: a) 1+3L 2-MOE; b) 1+3L PGME

4. Conclusions

Barium Zirconate Titanate – Barium Calcium Titanate thin films were successfully prepared by sol–gel technique in 2-methoxyethanol (2-MOE) and in a greener solvent such as 1-methoxy-2-propanol (PGME). After calcination both solutions resulted in a perovskite structure, even if their thermal behavior was different. 4-layer thin films were produced with a randomly oriented crystal structure and homogeneous nanometric grains. Nevertheless, some pores appear on the surface of the 2-MOE thin film.It can be concluded that both thin films are ferroelectric: the 2-MOE capacitor performs by 30% more with respect to PGME one also due to the 15% higher thickness. It implies that more layer have to be deposited in the case of PGME capacitor to have the same performances of 2-MOE one. Nevertheless, the use of non –toxic solvents is more auspicated, and this study demonstrate the feasibility of a sol-gel process with greener solvents.

References

Aprea P., Liguori B., Caputo D., Casuscelli V., Cimmino A., di Matteo A., Salzillo G., 2017, Green Chemical Routes for the Synthesis of Lead-Free Ferroelectric Material $0.5Ba(Zr_{0.2}Ti_{0.8})O_3$–$0.5(Ba_{0.7}Ca_{0.3})TiO_3$, Advanced Science Letters, 23, 6015-6019.

Barbato P. S., Aprea P., Caputo D., Casuscelli V., Scaldaferri R., di Matteo A., 2019, $0.5(BaZr_{0.2}Ti_{0.8}O_3)$-$0.5(Ba_{0.7}Ca_{0.3}O_3)$ thin films deriving from green sol-gel routes, IEEE 8th International Workshop on Advances in Sensors and Interfaces (IWASI), Otranto, Italy, 139-142.

Hu P., 2018, Study on high precision mems inertial sensor with increased detection capacitance driven by electromagnetism, Chemical Engineering Transactions, 66, 1273-1278.

Kang G., Yao K., Wang J., 2012, $(1−x)Ba(Zr_{0.2}Ti_{0.8})O_3$–$x(Ba_{0.7}Ca_{0.3})TiO_3$ ferroelectric thin films prepared from chemical solutions, Journal of American Ceramic Society, 95, 986-991.

Lin Y., Wu G., Qin N., Bao D., 2012, Structure, dielectric, ferroelectric, and optical properties of $(1−x)Ba(Zr_{0.2}Ti_{0.8})O_3$–$x(Ba_{0.7}Ca_{0.3})TiO_3$ thin films prepared by sol–gel method, Thin Solid Films, 520(7), 2800-2804.

Malič B., Kupec A., Vojisavljević K., Pečnik T., 2018, Lead-Free Ferroelectric Thin Films. In L. Klein et al. (Eds.), Handbook of Sol- Gel Science and Technology, Springer International Publishing.

Shen Y., Liu Y., 2018, Properties of piezoelectric ceramics nanofilm from sol-gel process, Chemical Engineering Transactions, 66, 61-66.

Trolier-McKinstry S., Muralt P., 2004, Thin Film Piezoelectrics for MEMS, Journal of Electroceramics, 12, 7–17.

Wang, Z., Zhao, K., Guo, X., Sun, W., Jiang, H., Han, X., Tao, X., Cheng, Z., Zhao, H., Kimura, H., Yuan, G., Yin, J. & Liu, Z.,2013.Crystallization, phase evolution and ferroelectric properties of sol-gel-synthesized $Ba(Ti_{0.8}Zr_{0.2})O_3$- $x(Ba_{0.7}Ca_{0.3})TiO_3$ thin films. Journal of Materials Chemistry C, 1, 522-530.